nature publishing group

Potential role of increased oxygenation in altering perinatal adrenal steroidogenesis

Vishal Agrawal[1], Meng Kian Tee[1], Jie Qiao[1], Marcus O. Muench[2,3] and Walter L. Miller[1]

BACKGROUND: At birth, the large fetal adrenal involutes rapidly, and the patterns of steroidogenesis change dramatically; the event(s) triggering these changes remain largely unexplored. Fetal abdominal viscera receive hypoxic blood having a partial pressure of oxygen of only ~2 kPa (20–23 mm Hg); perinatal circulatory changes change this to adult values (~20 kPa). We hypothesized that transition from fetal hypoxia to postnatal normoxia participates in altering perinatal steroidogenesis.

METHODS: We grew midgestation human fetal adrenal cells and human NCI-H295A adrenocortical carcinoma cells in 2% O_2, then transitioned them to 20% O_2 and quantitated steroidogenic mRNAs by quantitative PCR and microarrays.

RESULTS: Transitioning fetal adrenal cells from hypoxia to normoxia increased mRNAs for 17α-hydroxylase/17,20 lyase (P450c17), 3β-hydroxysteroid dehydrogenase (3βHSD2), and steroidogenic acute regulatory protein (StAR). We repeated the protocol with NCI-H295A cells acclimated to hypoxia for 15 d, quantitating 31,255 transcripts by microarray. Using an arbitrary 1.5-fold difference, 1 d of normoxia increased 4 transcripts and decreased 56, whereas 2 d of normoxia increased 62 transcripts and decreased 105. P450c17, 3βHSD2, and StAR were ranked among the top eight increased transcripts.

CONCLUSION: These data suggest that the hypoxic/normoxic transition at birth contributes to perinatal changes in adrenal steroidogenesis.

At birth, the transition from intrauterine to extrauterine life requires major endocrine adjustments, such as the metabolic adjustments following the discontinuation of glucose supplied from cord blood and the rapid shift from producing reverse T3 to T3. Understanding these transitions is essential in the endocrine care of the perinatal patient. Evaluation of newborn adrenal function is complicated by the fact that the fetal and later infant adrenals are very different. The human fetal adrenal has two zones, fetal and definitive, in contrast to the three zones, glomerulosa, fasciculata, and reticularis, of the adult gland. Fetal adrenal steroidogenesis begins at about 7 wk gestation: steroidogenic enzymes are detectable by immunocytochemistry in the fetal zone at 50–52 d postconception, and primary cultures of the 8 wk adrenal produce cortisol and respond to adrenocorticotropic hormone (1). The fetal adrenal transiently expresses 3β-hydroxysteroid dehydrogenase, type 2 (3βHSD2, encoded by *HSD3B2*) at about 8–10 wk, permitting fetal adrenal cortisol synthesis at the same time when male genital development occurs, thus helping to prevent the virilization of female fetuses by suppressing fetal adrenal androgen synthesis (1). The fetal adrenal has relatively little 3βHSD2 activity after 12 wk (1,2) but has 17α-hydroxylase and robust 17,20 lyase activity (both catalyzed by cytochrome P450c17, encoded by *CYP17A1*), considerable sulfotransferase activity, and little steroid sulfatase activity accounting for its abundant production of dehydroepiandrosterone (DHEA) and its sulfate (DHEAS). DHEAS is secreted, 16α-hydroxylated in the fetal liver by CYP3A7 (3–5), and then acted on by placental 3βHSD1, 17βHSD1 (17β-hydroxysteroid dehydrogenase type 1, encoded by *HSD17B1*), and aromatase (P450aro, encoded by *CYP19A1*) to produce estriol (6,7). Fetal adrenal steroids are the source of about half of the estrone and estradiol and 90% of the estriol in the maternal circulation (8). Despite the large amounts of DHEA and DHEAS produced by the fetal adrenal and their consequent metabolism to estrogens by the placenta, evidence for an essential role for these steroids is scant, as fetuses with genetic disorders of adrenal steroidogenesis develop normally, reach term gestation, and undergo normal parturition (9). Although glucocorticoids can induce premature lung maturation, they do not appear to be needed when human gestation goes to term, as complete absence of the glucocorticoid receptor is compatible with normal term birth and pulmonary function (10).

It has long been known that the adrenal grows rapidly throughout fetal life, reaching a combined weight of 8–9 g at birth (equal to the combined weight of the adult adrenals) (11–13), but within weeks of birth, the fetal adrenals involute to a total weight of about 2 g (12,14). This change is mediated by apoptosis of the fetal zone, possibly in response to activin A or transforming growth factor-β (15). In parallel with the involution of the fetal zone of the adrenal, secretion of DHEA and DHEAS falls dramatically (16–18). The triggering mechanism for this rapid, profound change in adrenal morphology, cellular architecture, and steroidogenesis is not known. It has been suggested that the involution of the fetal adrenal is more related to gestational age than to timing

The first two authors contributed equally to this work.

[1]Department of Pediatrics, University of California–San Francisco, San Francisco, California; [2]Blood Systems Research Institute, University of California–San Francisco, San Francisco, California; [3]Department of Laboratory Medicine, University of California–San Francisco, San Francisco, California. Correspondence: Walter L. Miller (wlmlab@ucsf.edu)

Received 9 June 2014; accepted 13 August 2014; advance online publication 24 December 2014. doi:10.1038/pr.2014.194

after birth (19), but more recent studies indicate that parturition itself triggers fetal adrenal involution, which was interpreted as suggesting that the withdrawal of a placental factor stimulated the onset of fetal adrenal apoptosis (20). We hypothesize that the transition from intrauterine hypoxia to extrauterine normoxia is also a key event in triggering the remodeling of the fetal adrenal. Human fetal abdominal viscera receive hypoxic blood having a partial pressure of oxygen (Po_2) of only ~2 kPa (1 kPa = 7.5 Torr; 1 Torr = 1 mm Hg); perinatal circulatory changes change this to adult values of ~20 kPa. As parturition itself appears to trigger the changes in fetal adrenal steroidogenesis and architecture, we considered whether the perinatal change in arterial oxygen tension participates in these changes. As a preliminary test of this hypothesis, we grew adrenal cells in long-term hypoxic conditions designed to mimic the intrauterine environment and then examined changes in gene expression upon transition to a normoxic environment that models extrauterine life.

RESULTS

Human Fetal Adrenal Cells

To study the changes in the human adrenal as it transitions from the hypoxia of fetal life to the normoxia of the extrauterine newborn environment, we first incubated adrenal cells from a single 17-wk human fetus under hypoxic conditions for 1 d, followed by normoxic conditions for 1 or 2 d. Total cellular RNA from these cells was hybridized to Illumina BeadChip microarrays for gene expression analyses. Using an arbitrary cutoff of >1.5-fold change for gene activation or <0.67-fold change for gene repression, the mRNAs encoded by 107 genes were increased, and those for 114 genes were decreased when the cells were shifted from fetal hypoxic conditions to normoxic conditions for 1 d, and 179 mRNAs were increased and 296 genes were decreased after 2 d in normoxic conditions (**Supplementary Tables S1 and S2** online). Of these transcripts, 54 were increased and 111 were decreased on both days (**Figure 1**).

While this experiment showed that the hypoxic–normoxic transition can change the abundance of many adrenal mRNAs, changes were not seen in the transcripts for any gene encoding a steroidogenic enzyme or its electron-transfer cofactor. To examine mRNAs encoding steroidogenic factors more closely, we obtained additional adrenals, incubated primary adrenal cell cultures under hypoxic and normoxic conditions, and measured the relative abundances of selected mRNAs under each condition for each adrenal by reverse transcription followed by quantitative real-time PCR. Consistent with prior observations (21), preliminary experiments showed that the relative abundances of mRNAs for P450scc and P450c17 decreased after 4 d due to the overgrowth of fibroblasts and apoptosis of fetal adrenal cells (data not shown). Thus, we used 2 d of culture for more detailed studies with adrenals from five fetuses (three male and two female; 17–23 wk gestation). We noted no changes in the morphology of the adrenal cells after transition from hypoxia to normoxia for 1–2 d. Under normoxic conditions, the abundance of the mRNAs for P450c17, steroidogenic acute regulatory protein (StAR), and 3βHSD2 increased after 2 d (**Figure 2**). Consistent with the data from other cell types (22), glyceraldehyde-3-phosphate dehydrogenase gene expression decreased in normoxia compared with hypoxia, but the expression of mRNAs for 3βHSD2, StAR, and P450c17 increased 2.6-, 2.0-, and 1.6-fold under normoxic conditions, while expression of P450scc barely changed. However, there was a substantial variation with the fetal adrenal cells from different fetuses, so that the statistical analyses were of marginal significance.

Human Adrenal NCI-H295A Cells

To avoid differences between individual fetal adrenals, we sought to use the immortalized human adrenal NCI-H295A cell line, in which the patterns of steroidogenesis closely

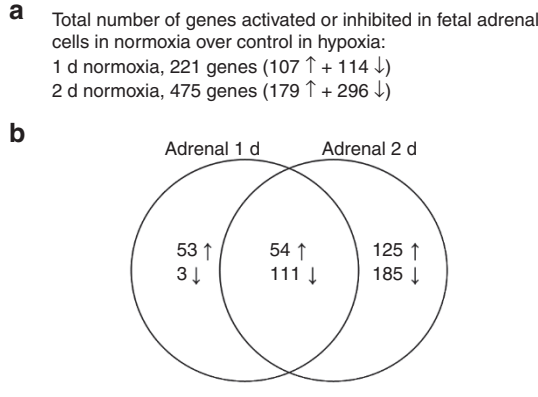

Figure 1. Summary of microarray gene expression profiles from the primary culture of human fetal adrenal cells. A primary culture of fetal adrenal cells was incubated under hypoxic conditions for 1 d, followed by normoxic conditions for either 1 or 2 d; control cells were maintained under hypoxic conditions throughout the experiment. (**a**) Gene expression levels were calculated as the signal levels under normoxic conditions divided by the signal levels under hypoxic conditions for control cells. (**b**) Venn diagram showing gene expression profiles in the primary culture of fetal adrenal cells incubated under the above conditions. Arrows pointing upward and downward represent increased and decreased numbers of expressed genes.

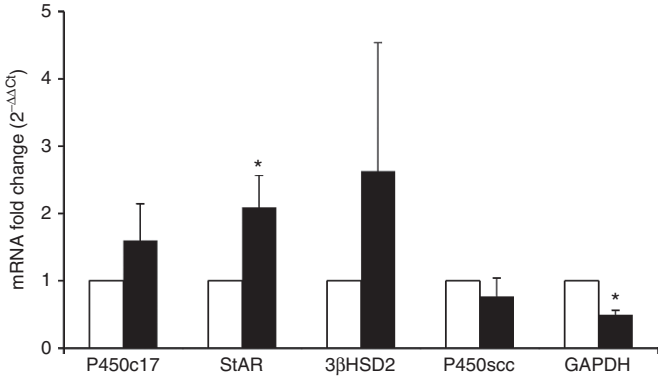

Figure 2. Expression of mRNAs in human fetal adrenal cells. Duplicate cultures of five fetal adrenals were grown in conditions of hypoxia (open bars) and normoxia (closed bars), and the mRNAs for P450c17, StAR, 3βHSD2, P450scc, and GAPDH were quantitated by qPCR. The mean levels in hypoxia are set at 100% for each RNA; data are mean ± SEM; *$P < 0.05$. 3βHSD2, 3β-hydroxysteroid dehydrogenase, type 2; GAPDH, glyceraldehyde-3-phosphate dehydrogenase; P450c17, 17α-hydroxylase/17,20 lyase; qPCR, quantitative PCR; StAR, steroidogenic acute regulatory protein.

resemble those of the fetal adrenal (23). Because these cells are normally cultured in normoxic conditions, we first acclimated them to the fetal environment by culturing them in hypoxic conditions for 15 d before "delivering" them to extrauterine normoxic conditions for either 1 or 2 d; control cells were maintained in hypoxic conditions throughout the experiment. We noted no changes in cellular morphology when the NCI-H295A cells were transitioned from 15 d of hypoxia to normoxia. The resulting mRNAs were analyzed by hybridization to Illumina BeadChip microarrays, thus permitting analysis of the entire transcriptome. In NCI-H295A cells, only 4 mRNAs were increased and 56 were decreased when the cells were shifted from fetal hypoxic conditions to extrauterine normoxic conditions for 1 d, and none of the altered mRNAs appeared to participate in steroidogenesis (**Table 1** and **Supplementary Table S3** online). By contrast, after the NCI-H295A cells had been returned to normoxia for 2 d, 62 mRNAs were increased and 105 mRNAs were decreased (**Table 2** and **Supplementary Table S3** online). Among the mRNAs that increased, three encode proteins that participate in steroidogenesis: P450c17 (*CYP17A1*), increased 1.65-fold; 3βHSD2 (*HSD3B2*), increased 1.89-fold; and StAR (*STAR*), increased 1.78-fold over controls. In addition, sterol isomerase (*EBP*), which participates in cholesterol biosynthesis, increased 1.57-fold. The degree of overlap in these gene populations is shown in **Figure 3**. These gene expression profiles showed that 46 mRNAs were regulated in the same fashion after both 1 and 2 days of normoxia (1 increased and 45 decreased). In addition, the mRNAs for 3 other genes were increased and 11 were decreased after 1 d of normoxia and 61 mRNAs were increased and 60 reduced after 2 d of normoxia.

Among the genes whose mRNAs increased or decreased under normoxic conditions (**Tables 1** and **2**), *ALDOA*, *ALDOC*, *BNIP3*, *BNIP3L*, *CA9*, *ENO1*, *GADPH*, *HK2*, *IGFBP2*, *JMJD1A*, *LDHA*, *NDRG1*, *PKM2*, *SLC2A1*, *SLC2A3*, and *TPI1* are known to be transcriptionally regulated by hypoxia (24). Only four genes, *BNIP3*, *NDRG1*, *SERPINA3*, and *SLC2A1* were regulated in common in both NCI-H295A cells and in the primary culture of fetal adrenal cells. The complete expression profile data for all genes in NCI-H295A and in the primary cultures of fetal adrenal cells are shown in **Supplementary Tables S1–S4** online.

Gene ontology analyses using Ingenuity Pathway Analysis (https://analysis.ingenuity.com) showed that many of the repressed genes in NCI-H295A incubated for 1 or 2 d in normoxic conditions participate in common pathways such as glycolysis, sucrose degradation, vitamin C transport, thyroid hormone receptor/retinoid X receptor activation, and HIF1α signaling (**Tables 3–5**). In contrast, the activated genes in NCI-H295A are involved in glutathione-mediated detoxification, dendritic-natural killer cells crosstalk, p53 signaling, and, of course, steroidogenesis.

DISCUSSION

Little information is available concerning the potential effects of environmental oxygenation on fetal adrenal function, and most such reports have investigated animal models of high-altitude stress. Thus, when pregnant rats were transitioned to reduced air pressure of ~380 Torr (~50 kPa; Po_2 ~10 kPa; designed to correspond to 18,000 feet above sea level), the adrenals of fetuses were larger, possibly due to increased adrenocorticotropic hormone secretion (25). Long-term maintenance of pregnant sheep at 3,820 m above sea level (Po_2 ~102 Torr; 13.6 kPa) reduced expression of mRNAs and proteins for P450scc, P450c17, and MC2R (adrenocorticotropic hormone receptor) but did not alter P450c21 (21-hydroxylase, encoded by *CYP21A2*), StAR (encoded by *STAR*), 3βHSD2, or DAX-1 (26). At birth, the fetal zone of the human adrenal cortex involutes rapidly, as evidenced by rapidly declining serum concentrations of DHEA and DHEAS. Furthermore, this rapid decline in DHEA/S is seen in both premature and term infants (27). Therefore, we and others have hypothesized that the involution of the fetal adrenal is not "programmed" but "triggered." A current view is that the trigger is the loss of placental hormones and growth factors (20). Such a trigger could also be secondary to the profound environmental change that accompanies birth. Such changes initiate the transition from fetal to postnatal circulatory patterns, including closure of the foramen ovale and the ductus arteriosus. Closure of the ductus is directly triggered by increased oxygen tension (via prostaglandins), and many other events in the newborn are triggered by the transition to normoxia (28). Thus, we hypothesized that the transition from the intrauterine hypoxic environment to the extrauterine normoxic environment might participate in initiating the rapid changes in adrenal steroidogenesis that follow birth. The fetal adrenal and other organs served by the fetal abdominal aorta are bathed in oxygen-poor blood having a partial pressure of oxygen of about 20–22 Torr (2.6–2.9 kPa) (29). Therefore, to model the changes in the adrenal environment that accompany birth, we incubated human fetal adrenal cells and human adrenal NCI-H295A cells in 2% oxygen (hypoxia, Po_2 ~2.0 kPa) followed by incubation in atmospheric oxygen (normoxia, ~20 kPa) for 1 and 2 d.

Results with human fetal adrenals suggested that the hypoxic–normoxic transition increased the mRNAs for StAR, 3βHSD2, and P450c17 and decreased the mRNA for P450scc, but only the data with StAR reached nominal significance of $P < 0.05$. There was substantial variation among adrenals from different donors, with no pattern attributable to donor sex or gestational age in the 17–23-wk period used. Therefore, we turned to human adrenocortical carcinoma NCI-H295A cells, which possess features typical of fetal, rather than adult, adrenal cells (e.g., expression of IGF-2 and P450aro) (23). The cells were propagated in hypoxic conditions for 15 d to acclimate them to this model intrauterine environment before "delivering" them to normoxia. This transition induced changes in the abundance of many mRNAs, with many more changes after 2 d than after 1 d. Not surprisingly, one of the induced genes was *HIF1A*, which encodes a hypoxia-induced transcription factor (30). Most notably, after 2 d of normoxia, the abundances of the mRNAs for the steroidogenic factors 3βHSD2, StAR, and P450c17 increased >1.6-fold. This will change the pattern of

Table 1. Expression of 4 genes activated and 56 genes inhibited in NCI-H295A cells incubated under hypoxic conditions for 15 d, followed by normoxic conditions for 1 d

Symbol	Gene	Mean ± SD[a]	Chromosome	Function
MIR1974	MicroRNA 1974	1.68 ± 1.26		MicroRNA
UCK2	Uridine-cytidine kinase 2	1.51 ± 0.16	1	Pyrimidine metabolism
AP1S1	Adaptor-related protein complex 1, sigma 1 subunit	1.50 ± 0.66	7	Protein sorting in the late-Golgi/trans-Golgi network and/or endosomes
GINS4	GINS complex subunit 4 (Sld5 homolog)	1.50 ± 0.67	8	Initiation of DNA replication and progression of DNA replication forks
PEG3	Paternally expressed 3	0.66 ± 0.10	19	Apoptosis
LOC100132564	Hypothetical protein LOC100132564	0.66 ± 0.27	12	Unknown
RNU1-3	U1 small nuclear 3	0.66 ± 0.22	1	Component of the spliceosome
SNORA28	Small nucleolar RNA, H/ACA box 28	0.66 ± 0.07	14	Unknown
NARF	Nuclear prelamin A recognition factor	0.66 ± 0.03	17	Binds to the prenylated prelamin A carboxyl-terminal tail domain
VIL2	Villin 2	0.66 ± 0.10	6	Actin cytoskeleton signaling
ANKRD37	Ankyrin repeat domain 37	0.65 ± 0.02	4	Unknown
MT1H	Metallothionein 1H	0.65 ± 0.18	16	Protein binding and zinc ion binding
LOC728188	Similar to phosphoglycerate mutase processed protein	0.65 ± 0.11	X	Unknown
WDR54	WD repeat domain 54	0.65 ± 0.07	2	Unknown
PGK1	Phosphoglycerate kinase 1	0.64 ± 0.06	X	Glycolysis/gluconeogenesis
MTP18	Mitochondrial protein 18 kDa	0.64 ± 0.04	22	Mitochondrial division
HIG-2	Hypoxia-inducible lipid droplet-associated	0.64 ± 0.02	7	Intracellular lipid accumulation
SNX26	Sorting nexin 26	0.63 ± 0.03	19	Intracellular trafficking
RNU1A3	RNA, U1A3 small nuclear	0.63 ± 0.20	1	Component of the spliceosome
SLC6A8	Solute carrier family 6 (neurotransmitter transporter, creatine), member 8	0.63 ± 0.10	X	Creatine uptake in muscles and brain
PGM1	Phosphoglucomutase 1	0.63 ± 0.07	1	Glycolysis/gluconeogenesis
PGAM1	Phosphoglycerate mutase 1 (brain)	0.63 ± 0.03	10	Glycolysis/gluconeogenesis
C4orf3	Chromosome 4 open reading frame 3	0.62 ± 0.05	4	Unknown
EZR	Ezrin	0.62 ± 0.09	6	Actin cytoskeleton signaling
PGAM1P8	Phosphoglycerate mutase 1 pseudogene 8	0.62 ± 0.06	11	Unknown
SLC2A3[b]	Solute carrier family 2 (facilitated glucose transporter), member 3	0.62 ± 0.03	12	Glucose transporter
ORM1	Orosomucoid 1	0.62 ± 0.03	9	Transport protein in the blood stream
GPI	Glucose phosphate isomerase	0.61 ± 0.06	19	Glycolysis/gluconeogenesis
LOC732165	Similar to triosephosphate isomerase (TIM) (triose-phosphate isomerase)	0.61 ± 0.07	1	Unknown
ADSSL1	Adenylosuccinate synthase like 1	0.60 ± 0.07	14	Component of the purine nucleotide cycle
MGC16121	Hypothetical protein MGC16121	0.60 ± 0.07	X	Unknown
GAPDH[b]	Glyceraldehyde-3-phosphate dehydrogenase	0.60 ± 0.06	12	Glycolysis/gluconeogenesis
EFHD2	EF-hand domain family, member D2	0.59 ± 0.04	1	Calcium ion binding, protein binding
TPI1[b]	Triosephosphate isomerase 1	0.59 ± 0.09	12	Glycolysis/gluconeogenesis
PNCK	Pregnancy upregulated nonubiquitously expressed CaM kinase	0.59 ± 0.12	X	Calcium signaling
TMEM45A	Transmembrane protein 45A	0.58 ± 0.07	3	Unknown
RN7SK	RNA, 7SK small nuclear	0.57 ± 0.19	6	Unknown
LOC732007	Similar to phosphoglycerate mutase 1 (phosphoglycerate mutase isozyme B) (PGAM-B) (BPG-dependent PGAM 1)	0.57 ± 0.08	12	Unknown

Table 1. Continued on next page

Table 1. Continued

Symbol	Gene	Mean ± SD[a]	Chromosome	Function
PLOD1	Procollagen-lysine 1, 2-oxoglutarate 5-dioxygenase 1	0.56 ± 0.09	1	Lysine degradation
JMJD1A[b]	Jumonji domain containing 1A	0.55 ± 0.06	2	Histone demethylation
ALDOA[b]	Aldolase A, fructose-bisphosphate	0.55 ± 0.06	16	Glycolysis and gluconeogenesis
TPI1P2	Triosephosphate isomerase 1 pseudogene 2	0.54 ± 0.01	7	Unknown
PFKP	Phosphofructokinase, platelet	0.53 ± 0.08	10	Fructose and mannose metabolism; galactose metabolism; glycolysis/ gluconeogenesis
SLC6A10P	Solute carrier family 6 (neurotransmitter transporter, creatine), member 10	0.52 ± 0.10	16	Unknown
ENO1[b]	Enolase 1, (alpha)	0.51 ± 0.04	1	Glycolysis/gluconeogenesis
TPI1P1	Triosephosphate isomerase 1 pseudogene 1	0.50 ± 0.06	1	Unknown
PKM2[b]	Pyruvate kinase, muscle	0.49 ± 0.08	15	Glycolysis/gluconeogenesis
BNIP3[b]	BCL2/adenovirus E1B 19 kDa interacting protein 3	0.49 ± 0.08	10	Nuclear gene encoding mitochondrial protein
SERPINA3	Serpin peptidase inhibitor, clade A (alpha-1 antiproteinase, antitrypsin), member 3	0.49 ± 0.11	14	Plasma protease inhibitor
BNIP3L[b]	BCL2/adenovirus E1B 19 kDa interacting protein 3-like	0.47 ± 0.01	8	Apoptosis
LOC644774	Similar to phosphoglycerate kinase 1	0.45 ± 0.02	X	Unknown
SPRR2F	Small proline-rich protein 2F	0.45 ± 0.11	1	Structural constituent of cytoskeleton
DDIT4	DNA-damage-inducible transcript 4	0.45 ± 0.09	10	Inhibits cell growth by regulating the mTOR signaling pathway
SLC2A1[b]	Solute carrier family 2 (facilitated glucose transporter), member 1	0.44 ± 0.03	1	Glucose transporter
ALDOC[b]	Aldolase C, fructose-bisphosphate	0.41 ± 0.07	17	Glycolysis and gluconeogenesis
LDHA[b]	Lactate dehydrogenase A	0.39 ± 0.04	11	Glycolysis/gluconeogenesis
NDRG1[b]	N-myc downstream regulated gene 1	0.36 ± 0.08	8	p53-mediated caspase activation and apoptosis
BHLHB2	Basic helix-loop-helix domain containing, class B, 2	0.35 ± 0.08	3	Transcriptional factor modulating chondrogenesis in response to the cAMP pathway
CYP2J2	Cytochrome P450, family 2, subfamily J, polypeptide 2	0.29 ± 0.06	1	Arachidonic acid metabolism; drug metabolism
PFKFB4	6-phosphofructo-2-kinase/fructose-2,6-biphosphatase 4	0.18 ± 0.05	3	Fructose and mannose metabolism

cAMP, cyclic adenosine monophosphate; mTOR, mammalian target of rapamycin.
[a]The data are expressed as mean fold change in normoxic conditions over control in hypoxic conditions ± SD. [b]Positive control genes known to be transcriptionally regulated by hypoxia.

steroidogenesis from Δ5 to Δ4 steroids, as is seen following birth.

Our study emphasizes analysis of mRNAs and did not measure the abundances of steroidogenic enzyme proteins or the steroid products of our adrenal cell systems; such measurements will be of interest in future studies. In addition, our experimental design only examined events in the first 2 d following the transition to normoxia, yet the involution of the fetal adrenal and the transition from fetal to newborn pattern of steroidogenesis takes several weeks, so that future studies may also examine a broader time frame. However, it seems likely that the rapid changes in oxygenation at delivery would constitute an acute trigger to change the adrenal's transcriptional programming and that such acute changes would subsequently affect adrenal morphology and steroid secretory patterns over the first weeks of life, so we would expect that the changes in mRNA abundances that we have measured would precede changes in adrenal morphology and steroid secretion. In this context, it may be important to add tropic activators of the protein kinase A pathway (adrenocorticotropic hormone to adrenal cells and 8-Br-cAMP to NCI-H295A cells), to mimic conditions *in vivo*.

Our data are consistent with our hypothesis that the change in oxygenation that follows birth is a key factor in determining the change in the patterns of adrenal steroidogenesis that follow birth. However, no aspect of our data is inconsistent with the hypothesis that withdrawal of placental factors also plays a role, especially in the rapid involution of adrenal size, as known adrenal growth factors (IGF-2, EGF, FGF) (31) were not among the factors dramatically changed by the hypoxic–normoxic transition in our studies. Thus, we propose that both the hypoxic–normoxic transition and the potential withdrawal of placental factors are required to initiate the anatomic

Table 2. Expression of 62 genes activated and 105 genes inhibited in NCI-H295A cells incubated under hypoxic conditions for 15 d, followed by normoxic conditions for 2 d

Symbol	Gene	Mean ± SD[a]	Chromosome	Function
PTMA	Prothymosin, alpha	2.31 ± 1.78	2	Mediate immune function
RPS2P28	Ribosomal protein S2 pseudogene 28	2.18 ± 0.64	6	Unknown
RPS3P3	Ribosomal protein S3 pseudogene 3	2.07 ± 0.86	3	Unknown
FLJ40504	Hypothetical protein FLJ40504	1.98 ± 0.40	17	Unknown
ID3	Inhibitor of DNA binding 3, dominant negative helix-loop-helix protein	1.91 ± 0.31	1	bHLH transcription factor binding
HSD3B2	Hydroxy-delta-5-steroid dehydrogenase, 3 beta- and steroid delta-isomerase 2	1.89 ± 0.57	1	Steroidogenesis
IGFBP2[b]	Insulin-like growth factor binding protein 2, 36 kDa	1.83 ± 0.28	2	IGF-1 signaling
StAR	Steroidogenic acute regulatory protein	1.78 ± 0.25	8	Steroidogenesis
PL6P10	Ribosomal protein L6 pseudogene 10	1.77 ± 1.09	4	Unknown
GSTA5	Glutathione *S*-transferase alpha 5	1.77 ± 0.13	6	Conjugation of reduced glutathiones and electrophiles
LOC651816	Similar to ubiquitin-conjugating enzyme E2S (ubiquitin-conjugating enzyme E2-24 kDa) (ubiquitin-protein ligase) (ubiquitin carrier protein) (E2-EPF5)	1.76 ± 0.52		Unknown
HLA-G	HLA-G histocompatibility antigen, class I, G	1.75 ± 0.76	6	Allograft rejection signaling; antigen presentation pathway
LOC644936	Cytoplasmic beta-actin pseudogene	1.75 ± 0.87	5	Unknown
LOC647169	Glutathione *S*-transferase alpha 3 pseudogene	1.74 ± 0.19	6	Unknown
FLJ20489	Hypothetical protein FLJ20489	1.72 ± 0.45	12	Unknown
KRT18P31	Keratin 18 pseudogene 31	1.70 ± 0.12	5	Unknown
RPS8P10	Ribosomal protein S8 pseudogene 10	1.70 ± 0.61	10	Unknown
FLJ43681	Ribosomal protein L23a pseudogene	1.68 ± 0.24	17	Unknown
KLK1	Kallikrein 1	1.65 ± 0.28	19	Serine protease
CYP17A1	Cytochrome P450, family 17, subfamily A, polypeptide 1	1.65 ± 0.32	10	Steroidogenesis
RPL23AP64	Ribosomal protein L23a pseudogene 64	1.64 ± 0.24	11	Unknown
CD9	CD9 molecule	1.64 ± 0.09	12	Platelet activation and aggregation, differentiation, adhesion, and signal transduction
PPPDE2	PPPDE peptidase domain containing 2	1.63 ± 0.40	22	Desumoylating isopeptidase
KRT18P59	Keratin 18 pseudogene 59	1.62 ± 0.28	11	Unknown
CCDC124	Coiled-coil domain containing 124	1.61 ± 0.48	19	DNA binding
KRT8	Keratin 8	1.60 ± 0.16	12	Cellular structural integrity, signal transduction, and cellular differentiation
MICA	MHC class I polypeptide-related sequence A	1.60 ± 0.18	6	Antigen processing and presentation
PERP	PERP, TP53 apoptosis effector	1.60 ± 0.46	6	p53 signaling
LOC728602	Ornithine decarboxylase antizyme 1 pseudogene	1.60 ± 0.48	1	Unknown
GSTA2	Glutathione *S*-transferase alpha 2	1.60 ± 0.25	6	Detoxification of electrophilic compounds
KRT18P13	Keratin 18 pseudogene 13	1.60 ± 0.17	9	Unknown
RPS2P51	Ribosomal protein S2 pseudogene 51	1.59 ± 0.32	19	Unknown
RPL18AP3	Ribosomal protein L18a pseudogene 3	1.59 ± 0.23	12	Unknown
RPL28P5	Ribosomal protein L28 pseudogene 5	1.58 ± 0.18	19	Unknown
UCK2	Uridine-cytidine kinase 2	1.58 ± 0.35	1	Pyrimidine metabolism
RPL7P32	Ribosomal protein L7 pseudogene 32	1.58 ± 0.02	7	Unknown
KRT8P47	Keratin 8 pseudogene 47	1.58 ± 0.07	1	Unknown
EBP	Emopamil-binding protein (sterol isomerase)	1.57 ± 0.54	X	Cholesterol biosynthesis

Table 2. Continued on next page

Table 2. Continued

Symbol	Gene	Mean ± SD[a]	Chromosome	Function
CKB	Creatine kinase, brain	1.57 ± 0.29	14	Transfer of phosphate between ATP and phosphogens
LOC730323	Hypothetical LOC730323	1.57 ± 0.70	7	Unknown
LOC389672	Similar to 40S ribosomal protein SA (p40) (34/67 kDa laminin receptor) (colon carcinoma laminin-binding protein) (NEM/1CHD4) (multidrug resistance-associated protein MGr1-Ag)	1.56 ± 0.47	8	Unknown
LOC649555	Similar to eukaryotic translation initiation factor 4E	1.56 ± 0.19	17	Unknown
CATSPER2	Cation channel, sperm associated 2	1.56 ± 0.77	15	Voltage-gated calcium channel
NOP16	NOP16 nucleolar protein homolog (yeast)	1.55 ± 0.16	5	Unknown
LOC100134053	Similar to POLR2J4 protein	1.55 ± 0.24	7	Unknown
XBP1	X-box binding protein 1	1.55 ± 0.18	22	Endoplasmic reticulum stress pathway
LOC100128098	Hypothetical protein LOC100128098	1.54 ± 0.64	10	Unknown
LOC642502	Succinate dehydrogenase complex, subunit C, integral membrane protein, 15 kDa pseudogene	1.54 ± 0.37	17	Unknown
HMGN2P25	High mobility group nucleosomal binding domain 2 pseudogene 25	1.53 ± 0.25	3	Unknown
PPIB	Peptidylprolyl isomerase B (cyclophilin B)	1.53 ± 0.20	15	Folding of proteins
LOC100129502	Hypothetical protein LOC100129502	1.53 ± 0.42	15	Unknown
SDF2L1	Stromal cell-derived factor 2-like 1	1.53 ± 0.21	22	Unknown
DCXR	Dicarbonyl/L-xylulose reductase	1.52 ± 0.15	17	Uronate cycle of glucose metabolism; osmoregulation in renal tubules
RPS26P35	Ribosomal protein S26 pseudogene 35	1.52 ± 0.24	8	Unknown
LOC651149	Similar to 60S ribosomal protein L3 (L4)	1.52 ± 0.09	10	Unknown
ADI1	Acireductone dioxygenase 1	1.52 ± 0.46	2	Catalyzes the formation of formate and 2-keto-4-methylthiobutyrate from 1,2-dihydroxy-3-keto-5-methylthiopentene
RPSAP56	Ribosomal protein SA pseudogene 56	1.51 ± 0.20	16	Unknown
RPS2P29	Ribosomal protein S2 pseudogene 29	1.51 ± 0.27	6	Unknown
CCT3	Chaperonin containing TCP1, subunit 3 (gamma)	1.51 ± 0.23	1	Molecular chaperone; assists the folding of proteins upon ATP hydrolysis
CDK5	Cyclin-dependent kinase 5	1.51 ± 0.31	7	Cell cycle
RPL29P15	Ribosomal protein L29 pseudogene 15	1.50 ± 0.32	5	Unknown
HIF1A	Hypoxia-inducible factor 1, alpha subunit	1.50 ± 0.45	14	Basic helix-loop-helix transcription factor activated in response to reduced oxygen availability in the cellular environment
SNORD13	Small nucleolar RNA, C/D box 13	0.66 ± 0.11	8	Unknown
MTMR11	Myotubularin-related protein 11	0.66 ± 0.06	1	Probable pseudophosphatase
MXD4	MAX dimerization protein 4	0.66 ± 0.04	4	Transcriptional repressor
KANK4	KN motif and ankyrin repeat domains 4	0.66 ± 0.14	1	Control of cytoskeleton formation by regulating actin polymerization
WDR54	WD repeat domain 54	0.66 ± 0.19	2	Unknown
RNU1G2	RNA, U1G2 small nuclear	0.65 ± 0.22	1	Unknown
MYLK4	Myosin light chain kinase family, member 4	0.65 ± 0.07	6	Protein serine/threonine kinase activity and ATP binding
HOXA5	Homeobox A5	0.65 ± 0.15	7	Transcription factor
MT1H	Metallothionein 1H	0.65 ± 0.06	16	Protein binding and zinc ion binding
RHBDL3	Rhomboid, veinlet-like 3 (*Drosophila*)	0.65 ± 0.05	17	Intramembrane proteolysis
GOLGA8B	Golgin A8 family, member B	0.64 ± 0.11	15	Maintaining Golgi structure
UBA7	Ubiquitin-like modifier activating enzyme 7	0.64 ± 0.04	3	Activates ubiquitin

Table 2. Continued on next page

Table 2. Continued

Symbol	Gene	Mean ± SD[a]	Chromosome	Function
C15orf52	Chromosome 15 open reading frame 52	0.64 ± 0.05	15	Unknown
PLOD2	Procollagen-lysine, 2-oxoglutarate 5-dioxygenase 2	0.64 ± 0.02	3	Lysine degradation
LOC286016	Triosephosphate isomerase 1 pseudogene	0.64 ± 0.14	7	Unknown
TAF1C	TATA box binding protein (TBP)-associated factor, RNA polymerase I, C, 110 kDa	0.64 ± 0.02	16	Component of the transcription factor SL1/TIF-IB complex
PHKA2	Phosphorylase kinase, alpha 2 (liver)	0.64 ± 0.04	X	Catalyzes serine phosphorylation
IL11RA	Interleukin 11 receptor, alpha	0.64 ± 0.03	9	Receptor for interleukin-11
SLC6A8	Solute carrier family 6 (neurotransmitter transporter, creatine), member 8	0.64 ± 0.10	X	Creatine uptake in muscles and brain
TPI1P1	Triosephosphate isomerase 1 pseudogene 1	0.64 ± 0.10	1	Unknown
ALDOA[b]	Aldolase A, fructose-bisphosphate	0.64 ± 0.07	16	Glycolysis and gluconeogenesis
GPI	Glucose phosphate isomerase	0.64 ± 0.03	19	Glycolysis/gluconeogenesis; pentose phosphate pathway; starch and sucrose metabolism
SNORD3A	Small nucleolar RNA, C/D box 3A	0.63 ± 0.11	17	Unknown
KLHL3	Kelch-like 3 (*Drosophila*)	0.63 ± 0.02	5	Substrate-specific adapter of a BTB-CUL3-RBX1 E3 ubiquitin ligase complex
DDIT4L	DNA-damage-inducible transcript 4-like	0.63 ± 0.07	4	Inhibits cell growth by regulating the mTOR signaling pathway
DPYSL4	Dihydropyrimidinase-like 4	0.63 ± 0.03	10	Signaling by class 3 semaphorins and subsequent remodeling of the cytoskeleton
KLF2	Kruppel-like factor 2 (lung)	0.63 ± 0.04	19	Binds CACCC box in the beta-globin gene promoter and activates transcription
RNU6-1	RNA, U6 small nuclear 1	0.63 ± 0.17	15	Unknown
COL11A1	Collagen, type XI, alpha 1	0.63 ± 0.08	1	Fibrillogenesis
APBB3	Amyloid beta (A4) precursor protein-binding, family B, member 3	0.63 ± 0.04	5	Internalization of beta-amyloid precursor protein
ZSWIM8	ZSWIM8 zinc finger, SWIM-type containing 8	0.63 ± 0.04	10	Unknown
PAM	Peptidylglycine alpha-amidating monooxygenase	0.63 ± 0.02	5	Catalyzes C-terminal alpha-amidation of peptides
MLLT6	Myeloid/lymphoid or mixed-lineage leukemia (trithorax homolog, *Drosophila*); translocated to, 6	0.62 ± 0.07	17	Unknown
ANKRD37	Ankyrin repeat domain 37	0.62 ± 0.05	4	Unknown
ZNF395	Zinc finger protein 395	0.62 ± 0.04	8	Unknown
SNORD113-5	Small nucleolar RNA, C/D box 113-5	0.62 ± 0.05	14	Unknown
ABP1	Amiloride binding protein 1 (amine oxidase (copper-containing)	0.62 ± 0.14	7	Degradation of putrescine, histamine, spermine, and spermidine
ZBTB40	Zinc finger and BTB domain containing 40	0.62 ± 0.07	1	Unknown
TMEM123	Transmembrane protein 123	0.61 ± 0.17	11	Oncotic cell death
RN5S9	RNA, 5S ribosomal 9	0.61 ± 0.27	1	Unknown
RNU1F1	RNA, U1F1 small nuclear	0.61 ± 0.22	14	Component of the spliceosome
WDR90	WD repeat domain 90	0.61 ± 0.07	16	Unknown
RNU6-15	RNA, U6 small nuclear 15	0.61 ± 0.15	—	Unknown
CLCNKA	Chloride channel Ka	0.60 ± 0.01	1	Voltage-gated chloride channel
SNORD3C	Small nucleolar RNA, C/D box 3C	0.60 ± 0.12	17	Unknown
SIRPA	Signal-regulatory protein alpha	0.60 ± 0.07	20	Immunoglobulin-like cell surface receptor for CD47
TPI1[b]	Triosephosphate isomerase 1	0.60 ± 0.04	12	Unknown
SLC27A3	Solute carrier family 27 (fatty acid transporter), member 3	0.60 ± 0.09	1	Acyl-CoA ligase activity

Table 2. Continued on next page

Table 2. Continued

Symbol	Gene	Mean ± SD[a]	Chromosome	Function
CLCN7	Chloride channel 7	0.60 ± 0.07	16	Antiporter; contributes to the acidification of the lysosome lumen
TMEM45A	Transmembrane protein 45A	0.60 ± 0.12	3	Unknown
COL3A1	Collagen, type III, alpha 1	0.60 ± 0.09	2	Regulation of cortical development
RNU1A3	RNA, U1A3 small nuclear	0.59 ± 0.26	1	Component of the spliceosome
JMJD1A[b]	Jumonji domain containing 1A	0.59 ± 0.08	2	Histone demethylation
SNORD3D	Small nucleolar RNA, C/D box 3D (SNORD3D)	0.59 ± 0.19	17	Unknown
PPP1R3C	Protein phosphatase 1, regulatory (inhibitor) subunit 3C	0.59 ± 0.12	10	Glycogen-targeting subunit for protein phosphatase 1
COL7A1	Collagen, type VII, alpha 1 (epidermolysis bullosa, dystrophic, dominant and recessive)	0.59 ± 0.03	3	Stratified squamous epithelial basement membrane protein that forms anchoring fibrils
LOC100132564	Hypothetical protein LOC100132564	0.59 ± 0.23	12	Unknown
PGK1	Phosphoglycerate kinase 1	0.58 ± 0.11	X	Glycolysis/gluconeogenesis
LOC100132394	Hypothetical protein LOC100132394	0.58 ± 0.22	X	Unknown
CYP1A1	Cytochrome P450, family 1, subfamily A, polypeptide 1	0.58 ± 0.04	15	Xenobiotic metabolism
RAP1GAP	RAP1 GTPase activating protein	0.58 ± 0.03	1	GTPase activator
ALKBH5	AlkB, alkylation repair homolog 5 (*E. coli*)	0.57 ± 0.02	17	Demethylation of RNA by oxidative demethylation
SVEP1	Sushi, von Willebrand factor type A, EGF and pentraxin domain containing 1	0.57 ± 0.06	9	Cell attachment process
SCGB1D2	Secretoglobin, family 1D, member 2	0.57 ± 0.07	11	Bind androgens and other steroids
TMEM145	Transmembrane protein 145	0.56 ± 0.10	19	Unknown
SLC2A3[b]	Solute carrier family 2 (facilitated glucose transporter), member 3	0.56 ± 0.05	12	Glucose transporter
FAM62B	Family with sequence similarity 62 (C2 domain containing) member B	0.56 ± 0.00	7	Calcium-regulated intrinsic membrane protein
LOC644774	Similar to phosphoglycerate kinase 1	0.56 ± 0.04	X	Unknown
RNU1-3	RNA, U1 small nuclear 3	0.56 ± 0.24	1	Component of the spliceosome
SLC6A10P	Solute carrier family 6 (neurotransmitter transporter, creatine), member 10 (pseudogene)	0.56 ± 0.09	16	Unknown
RNU1-5	RNA, U1 small nuclear 5	0.56 ± 0.24	1	Component of the spliceosome
[b]HK2	Hexokinase 2	0.56 ± 0.03	2	Aminosugars metabolism; fructose and mannose metabolism; galactose metabolism; glycolysis/gluconeogenesis
MT1F	Metallothionein 1F	0.56 ± 0.08	16	Cadmium ion binding and copper ion binding
STK36	Serine/threonine kinase 36, fused homolog (*Drosophila*)	0.56 ± 0.02	2	Sonic hedgehog signaling
COL22A1	Collagen, type XXII, alpha 1	0.55 ± 0.06	8	Cell adhesion ligand for skin epithelial cells and fibroblasts
MST1	Macrophage stimulating 1 (hepatocyte growth factor-like)	0.55 ± 0.03	3	IL-12 signaling and production in macrophages; MSP-RON signaling pathway
PKM2[b]	Pyruvate kinase, muscle	0.54 ± 0.05	15	Glycolysis/gluconeogenesis
PFKP	Phosphofructokinase, platelet	0.54 ± 0.07	10	Fructose and mannose metabolism; galactose metabolism; glycolysis/gluconeogenesis
ARHGEF16	Rho guanine exchange factor (GEF) 16	0.54 ± 0.05	1	Guanyl-nucleotide exchange factor activity
PNCK	Pregnancy upregulated nonubiquitously expressed CaM kinase	0.54 ± 0.08	X	Calcium signaling
ADSSL1	Adenylosuccinate synthase like 1	0.54 ± 0.07	14	Alanine and aspartate metabolism; purine metabolism
ENO1[b]	Enolase 1, (alpha)	0.53 ± 0.04	1	Glycolysis/gluconeogenesis

Table 2. Continued on next page

Table 2. Continued

Symbol	Gene	Mean ± SD[a]	Chromosome	Function
SSPO	SCO-spondin homolog (*Bos taurus*)	0.53 ± 0.05	7	Modulation of neuronal aggregation
PGM1	Phosphoglucomutase 1	0.51 ± 0.05	1	Glycolysis/gluconeogenesis
SNX26	Sorting nexin 26	0.51 ± 0.09	19	Intracellular trafficking
MGC16121	Hypothetical protein MGC16121	0.51 ± 0.08	X	Unknown
VIL2	Villin 2 (ezrin)	0.51 ± 0.07	6	Actin cytoskeleton signaling
EFHD2	EF-hand domain family, member D2	0.51 ± 0.04	1	Calcium ion binding, protein binding
RFTN1	Raftlin, lipid raft linker 1	0.51 ± 0.02	3	Formation and/or maintenance of lipid rafts
EZR	Ezrin	0.50 ± 0.11	6	Actin cytoskeleton signaling
DDIT4	DNA-damage-inducible transcript 4	0.49 ± 0.09	10	Inhibits cell growth by regulating the mTOR signaling pathway
SLC2A1[b]	Solute carrier family 2 (facilitated glucose transporter), member 1	0.47 ± 0.03	1	Glucose transporter
PLOD1	Procollagen-lysine 1, 2-oxoglutarate 5-dioxygenase 1	0.47 ± 0.05	1	Lysine degradation
BNIP3[b]	BCL2/adenovirus E1B 19 kDa interacting protein 3	0.47 ± 0.08	10	Apoptosis
RN7SK	RNA, 7SK small nuclear	0.43 ± 0.18	6	Pre-mRNA splicing and processing
LDHA[b]	Lactate dehydrogenase A	0.43 ± 0.02	11	Glycolysis/gluconeogenesis
BNIP3L[b]	BCL2/adenovirus E1B 19 kDa interacting protein 3-like	0.41 ± 0.02	8	Apoptosis
RNU4-2	RNA, U4 small nuclear 2	0.41 ± 0.19		Pre-mRNA splicing and processing
ALDOC[b]	Aldolase C, fructose-bisphosphate	0.41 ± 0.12	17	Glycolysis and gluconeogenesis
ORM1	Orosomucoid 1	0.39 ± 0.09	9	Transport protein in the blood stream
SERPINA3	Serpin peptidase inhibitor, clade A (alpha-1 antiproteinase, antitrypsin), member 3	0.33 ± 0.08	14	Plasma protease inhibitor
BHLHB2	Basic helix-loop-helix domain containing, class B, 2	0.32 ± 0.09	3	Transcriptional factor modulating chondrogenesis in response to the cAMP pathway
NDRG1[b]	N-myc downstream regulated gene 1	0.26 ± 0.05	8	p53-mediated caspase activation and apoptosis
CYP2J2	Cytochrome P450, family 2, subfamily J, polypeptide 2	0.23 ± 0.06	1	Arachidonic acid metabolism; drug metabolism
PFKFB4	6-phosphofructo-2-kinase/fructose-2,6-biphosphatase 4	0.16 ± 0.05	3	Fructose and mannose metabolism

cAMP, cyclic adenosine monophosphate; mTOR, mammalian target of rapamycin.
[a]The data are expressed as mean fold change in normoxic conditions over control in hypoxic conditions ± SD. [b]Positive control genes known to be transcriptionally regulated by hypoxia.

Table 3. Pathway analysis of genes downregulated in NCI-H295A cells incubated in hypoxic conditions for 15 d, followed by normoxic conditions for 1 d

Canonical pathways	*P* value	Molecules
Glycolysis	2.51×10^{-23}	PGK1, ENO1, GPI, TPI1, PGAM1, PKM2, GAPDH, ALDOA, PFKP, ALDOC
Sucrose degradation	3.55×10^{-7}	TPI1, ALDOA, ALDOC
Vitamin C transport	2.29×10^{-3}	SLC2A1, SLC2A3
TR/RXR activation	3.80×10^{-3}	ENO1, SLC2A1, PFKP
HIF1α signaling	5.50×10^{-3}	SLC2A1, LDHA, SLC2A3

TR/RXR, thyroid hormone receptor/retinoid X receptor.

remodeling of the fetal adrenal and its change in steroidogenic patterns as the fetus transitions to extrauterine life. While there may be differences among expression levels of mRNAs, their encoded proteins, and downstream steroids, our preliminary data suggest that the hypoxic/normoxic transition at birth is likely to be an important component of the perinatal changes in adrenal architecture and steroidogenesis.

METHODS

Cells

We used two cell systems. First, we used primary cultures from human fetal adrenals obtained with written consent from women undergoing elective procedures at San Francisco General Hospital. This research was performed with Institutional Review Board approval from the University of California San Francisco's Committee on Human Research. All specimens were anonymous. The gestational age of the fetal specimens was estimated based on foot length. Second, we used the NCI-H295A human adrenocortical cell line (32) that expresses all adrenal steroidogenic enzymes (23) and has been selected to grow in monolayer (33). All cells were grown in Roswell Park Memorial Institute (RPMI) medium (UCSF cell culture facility) with 2% fetal bovine serum. All experiments were performed in triplicate. Hypoxic conditions consisted of an atmosphere of 2% oxygen, 93% nitrogen, and 5% CO_2 in the XVIVO hypoxia tissue culture hood from

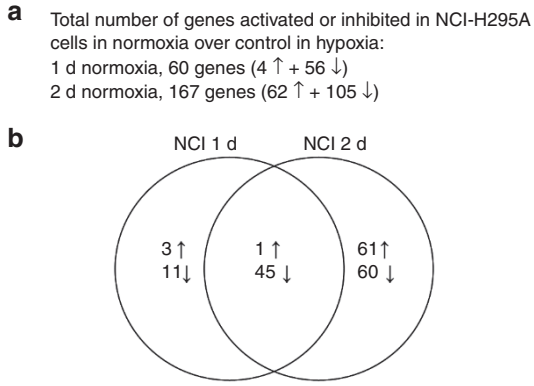

Figure 3. Summary of microarray gene expression profiles from NCI-H295A cells. NCI-H295A cells were incubated under hypoxic conditions for 15 d, followed by normoxic conditions for either 1 d or 2 d, while control cells were maintained under hypoxic conditions throughout the experiment. (**a**) Gene expression levels were calculated as the signal levels under normoxic conditions divided by the signal levels under hypoxic conditions for control cells. A fold change cutoff of >1.5-fold or <0.67-fold over control was chosen in our study. (**b**) Venn diagram showing gene expression profiles in NCI-H295A cells incubated under the above conditions. Arrows pointing upward and downward represent increased and decreased gene expression.

Table 4. Pathway analysis of genes upregulated in NCI-H295A cells incubated in hypoxic conditions for 15 d, followed by normoxic conditions for 2 d

Canonical pathways	*P* value	Molecules
Glutathione-mediated detoxification	2.04×10^{-7}	GSTA2, GSTA5
Steroidogenesis	8.51×10^{-7}	CYP17A1, EBP, HSD3B2, StAR
Crosstalk between dendritic cells and natural killer cells	3.63×10^{-3}	HLA-G, MICA
p53 signaling	4.37×10^{-2}	PERP, HIF1A

Table 5. Pathway analysis of genes downregulated in NCI-H295A cells incubated in hypoxic conditions for 15 d, followed by normoxic conditions for 2 d

Canonical pathways	*P* value	Molecules
Glycolysis	3.16×10^{-12}	PGK1, ENO1, GPI, TPI1, PKM2, ALDOA, PFKP, ALDOC
Sucrose degradation	4.47×10^{-6}	TPI1, ALDOA, ALDOC
Systemic lupus erythematosus signaling	6.17×10^{-4}	RNU1-3, RNU4-2, RNU6-1
Estrogen biosynthesis	3.31×10^{-3}	CYP1A1, CYP2J2
Vitamin C transport	7.76×10^{-3}	SLC2A1, SLC2A3
TR/RXR activation	2.09×10^{-2}	ENO1, SLC2A1, PFKP
HIF1α signaling	2.95×10^{-2}	SLC2A1, LDHA, SLC2A3

TR/RXR, thyroid hormone receptor/retinoid X receptor.

BioSpherix (Lacona, NY). Constant oxygen levels were maintained in the hypoxia chamber throughout the experimental procedure and incubations. All plastic ware, pipette aids, tissue culture media, and buffers were equilibrated in the hypoxic conditions before use.

Incubations

Under an institutional review board–approved human experimentation protocol, fetal adrenal tissues was transported in a full tube of phosphate-buffered saline that had been degassed so as to minimize exposure to oxygen before arriving in the laboratory. All manipulations were done under hypoxic conditions. Fetal adrenals were decapsulated, the two adrenals were combined, minced into small pieces, rinsed twice with Ca/Mg-free Hank's balanced salt solution, digested with 44 mg dispase (Life Technologies, Carlsbad, CA), 20 mg collagenase type I (Worthington Biochemical, Lakewood, NJ) at 37°C for 40 min, filtered through 100 μm nylon mesh, layered onto 5 ml ficoll-paque plus (GE Healthcare, Piscataway, NJ), and centrifuged at 600*g* for 30 min at room temperature on an IEC centraGP8R centrifuge (Thermo Fisher Scientific, Waltham, MA). The cells from the resulting interphase was collected and washed, resuspended in RPMI medium, and incubated in the hypoxic environment. Cells from each fetus were incubated separately in duplicate cultures grown in hypoxic or normoxic conditions; subsequent RNA preparations and analyses were done separately.

NCI-H295A cells were incubated under hypoxic conditions for 15 d and were split twice before the start of the experiment. After 15 d, six 10-cm plates of cells were moved from hypoxic conditions to an incubator with room air (normoxia). RNA was isolated from three plates after 1 d in normoxia and from the other three plates after 2 d in normoxia. RNA was also isolated from three control plates maintained in hypoxia.

Table 6. Sequence of primers used for qRT-PCR

Name	Sequence	Size of product (bp)
CYP11A1 forward	5′- TCC AGA AGT ATG GCC CGATT -3′	75
CYP11A1 reverse	5′- CAT CTT CAG GGT CGATGA CAT AAA -3′	
CYP17A1 forward	5′- TCT CTG GGC GGC CTC AA -3′	63
CYP17A1 reverse	5′- AGG CGATAC CCT TAC GGTTGT -3′	
HSD3B2 forward	5′- GGA AGA GAA GGA ACT GAA GGA G -3′	194
HSD3B2 reverse	5′- AGA CAT CAATGA TAC AGG CGG -3′	
StAR forward	5′- CCA CCC CTA GCA CGT GGAT -3′	88
StAR reverse	5′-TCCTGGTCA CTG TAG AGA GTC TCT TC -3′	
GAPDH forward	5′- CGG GGCTCT CCA GAA CAT CAT CC -3′	199
GAPDH reverse	5′- CGA CGC CTG CTT CAC CAC CTT CTT -3′	
ACTIN forward	5′- AACTCCATCATGAAGTGTGACG -3′	234
ACTIN reverse	5′- GATCCACATCTGCTGGAAGG -3′	

qRT-PCR, quantitative reverse transcription PCR.

RNA Analysis

Total RNA was isolated using TRIzol (Life Technologies) according to the manufacturer's recommended protocol. For cells kept in hypoxia, homogenization with TRIzol was done under hypoxic conditions. RNA was quantitated using an ND-1000 NanoDrop spectrophotometer (Thermo Scientific).

For real-time quantitative reverse transcription-PCR, 1 μg total RNA was reverse transcribed using Superscript II reverse transcriptase (Life Technologies), and PCR was performed at 94 °C for 5 min, followed by 40 cycles of 94 °C for 0.5 min, 55 °C for 0.5 min, and 72 °C for 1 min using primers and probes for the cholesterol side-chain cleavage enzyme (P450scc, encoded by *CYP11A1*), P450c17, 3βHSD2, StAR, glyceraldehyde-3-phosphate dehydrogenase, and actin (Table 6). Reactions were performed in a total volume 25 μl containing 2 μl complementary DNA and 12.5 μl FastStart SYBR Green Master (Roche, Mannheim, Germany) on an iCycler iQ Real Time Detection System (Bio-Rad, Hercules, CA).

For microarray experiments, 300 ng total RNA was used to produce biotin-labeled complementary RNA using Illumina TotalPrep RNA amplification kit (Life Technologies) according to the manufacturer's recommended protocol. The biotinylated complementary

RNA was eluted in nuclease-free water and was quantitated by NanoDrop spectrophotometer. Hybridization to the HumanHT-12 v4 BeadChip array (Illumina, San Diego, CA) was done at a complementary RNA concentration of 150 ng/μl in the UCSF Genomic Core Facility. The chips were scanned, and data were analyzed using Genome Studio Gene Expression Module (Illumina). Data were normalized using the "quantile" method of normalization in the software. Normalized data containing the signal levels and detection *P* values were exported into Microsoft Excel for gene expression analysis. The fold changes in gene expression levels were calculated as the gene signal levels under normoxic conditions divided by the signal levels under hypoxic conditions for control cells. The data are expressed as mean fold change in normoxia over control in hypoxia ± SD. Genes with signal detection of $P > 0.05$ in both normoxia and control groups were excluded from further analysis. An arbitrary fold change cutoff of >1.5-fold or <0.67-fold over control was chosen.

SUPPLEMENTARY MATERIAL

Supplementary material is linked to the online version of the paper at http://www.nature.com/pr

ACKNOWLEDGMENTS

We thank Emin Maltepe for productive discussions and for the use of the hypoxia chamber, Marcus Schoneman for helpful advice, and the staff and faculty at San Francisco General Hospital Women's Options Center for assistance in the collection of human fetal tissues. V.A. is currently Assistant Professor, Centre for Microbial Biotechnology, Panjab University, Chandigarh, India.

STATEMENT OF FINANCIAL SUPPORT

This work was supported by the University of California–San Francisco Molecular Endocrinology Fund; J.Q. was supported by the School of Medicine, Shanghai Jiao Tong University, Shanghai, China.

Disclosure: The authors have nothing to disclose. The authors report no conflict of interest.

REFERENCES

1. Goto M, Piper Hanley K, Marcos J, et al. In humans, early cortisol biosynthesis provides a mechanism to safeguard female sexual development. J Clin Invest 2006;116:953–60.
2. Voutilainen R, Ilvesmäki V, Miettinen PJ. Low expression of 3 β-hydroxy-5-ene steroid dehydrogenase gene in human fetal adrenals in vivo; adrenocorticotropin and protein kinase C-dependent regulation in adrenocortical cultures. J Clin Endocrinol Metab 1991;72:761–7.
3. Kitada M, Kamataki T, Itahashi K, Rikihisa T, Kanakubo Y. P-450 HFLa, a form of cytochrome P-450 purified from human fetal livers, is the 16 α-hydroxylase of dehydroepiandrosterone 3-sulfate. J Biol Chem 1987;262:13534–7.
4. Miller KK, Cai J, Ripp SL, Pierce WM Jr, Rushmore TH, Prough RA. Stereo- and regioselectivity account for the diversity of dehydroepiandrosterone (DHEA) metabolites produced by liver microsomal cytochromes P450. Drug Metab Dispos 2004;32:305–13.
5. Leeder JS, Gaedigk R, Marcucci KA, et al. Variability of CYP3A7 expression in human fetal liver. J Pharmacol Exp Ther 2005;314:626–35.
6. Kari MA, Raivio KO, Stenman UH, Voutilainen R. Serum cortisol, dehydroepiandrosterone sulfate, and steroid-binding globulins in preterm neonates: effect of gestational age and dexamethasone therapy. Pediatr Res 1996;40:319–24.
7. Miller WL. Steroid hormone biosynthesis and actions in the materno-feto-placental unit. Clin Perinatol 1998;25:799–817, v.
8. Siiteri PK, MacDonald PC. Placental estrogen biosynthesis during human pregnancy. J Clin Endocrinol Metab 1966;26:751–61.
9. Miller WL, Auchus RJ. The molecular biology, biochemistry, and physiology of human steroidogenesis and its disorders. Endocr Rev 2011;32:81–151.
10. McMahon SK, Pretorius CJ, Ungerer JP, et al. Neonatal complete generalized glucocorticoid resistance and growth hormone deficiency caused by a novel homozygous mutation in helix 12 of the ligand binding domain of the glucocorticoid receptor gene (NR3C1). J Clin Endocrinol Metab 2010;95:297–302.
11. Keene MF. Observations on the development of the human suprarenal gland. J Anat 1927;61(Pt 3):302–24.
12. Lanman JT. The fetal zone of the adrenal gland: its developmental course, comparative anatomy, and possible physiologic functions. Medicine (Baltimore) 1953;32:389–430.
13. Villee DB. The development of steroidogenesis. Am J Med 1972;53:533–44.
14. McNutt NS, Jones AL. Observations on the ultrastructure of cytodifferentiation in the human fetal adrenal cortex. Lab Invest 1970;22:513–27.
15. Spencer SJ, Mesiano S, Lee JY, Jaffe RB. Proliferation and apoptosis in the human adrenal cortex during the fetal and perinatal periods: implications for growth and remodeling. J Clin Endocrinol Metab 1999;84:1110–5.
16. Sucheston ME, Cannon MS. Development of zonular patterns in the human adrenal gland. J Morphol 1968;126:477–91.
17. Kojima S, Yanaihara T, Nakayama T. Serum steroid levels in children at birth and in early neonatal period. Am J Obstet Gynecol 1981;140:961–5.
18. Grueters A, Korth-Schutz S. Longitudinal study of plasma dehydroepiandrosterone sulfate in preterm and fullterm infants. J Clin Endocrinol Metab 1982;55:314–20.
19. Midgley PC, Russell K, Oates N, Holownia P, Shaw JC, Honour JW. Adrenal function in preterm infants: ACTH may not be the sole regulator of the fetal zone. Pediatr Res 1998;44:887–93.
20. Ben-David S, Zuckerman-Levin N, Epelman M, et al. Parturition itself is the basis for fetal adrenal involution. J Clin Endocrinol Metab 2007;92:93–7.
21. Di Blasio AM, Voutilainen R, Jaffe RB, Miller WL. Hormonal regulation of messenger ribonucleic acids for P450scc (cholesterol side-chain cleavage enzyme) and P450c17 (17 α-hydroxylase/17,20-lyase) in cultured human fetal adrenal cells. J Clin Endocrinol Metab 1987;65:170–5.
22. Higashimura Y, Nakajima Y, Yamaji R, et al. Up-regulation of glyceraldehyde-3-phosphate dehydrogenase gene expression by HIF-1 activity depending on Sp1 in hypoxic breast cancer cells. Arch Biochem Biophys 2011;509:1–8.
23. Staels B, Hum DW, Miller WL. Regulation of steroidogenesis in NCI-H295 cells: a cellular model of the human fetal adrenal. Mol Endocrinol 1993;7:423–33.
24. Halle C, Andersen E, Lando M, et al. Hypoxia-induced gene expression in chemoradioresistant cervical cancer revealed by dynamic contrast-enhanced MRI. Cancer Res 2012;72:5285–95.
25. Holland RC. The effect of hypoxia on the fetal rat adrenal. Anat Rec 1958;130:177–95.
26. Myers DA, Hyatt K, Mlynarczyk M, Bird IM, Ducsay CA. Long-term hypoxia represses the expression of key genes regulating cortisol biosynthesis in the near-term ovine fetus. Am J Physiol Regul Integr Comp Physiol 2005;289:R1707–14.
27. Honour JH, Wickramaratne K, Valman HB. Adrenal function in preterm infants. Biol Neonate 1992;61:214–21.
28. Dunwoodie SL. The role of hypoxia in development of the mammalian embryo. Dev Cell 2009;17:755–73.
29. Rudolph AM. Fetal circulation and cardiovascular adjustments after birth. In: Rudolph AM, Hoffman JIE, Rudolph CD, eds. Rudolph's Pediatrics, 20th edn. Stamford, CT: Appleton & Lange, 1996:1409–13.
30. Park AM, Sanders TA, Maltepe E. Hypoxia-inducible factor (HIF) and HIF-stabilizing agents in neonatal care. Semin Fetal Neonatal Med 2010;15:196–202.
31. Mesiano S, Mellon SH, Jaffe RB. Mitogenic action, regulation, and localization of insulin-like growth factors in the human fetal adrenal gland. J Clin Endocrinol Metab 1993;76:968–76.
32. Gazdar AF, Oie HK, Shackleton CH, et al. Establishment and characterization of a human adrenocortical carcinoma cell line that expresses multiple pathways of steroid biosynthesis. Cancer Res 1990;50:5488–96.
33. Rodriguez H, Hum DW, Staels B, Miller WL. Transcription of the human genes for cytochrome P450scc and P450c17 is regulated differently in human adrenal NCI-H295 cells than in mouse adrenal Y1 cells. J Clin Endocrinol Metab 1997;82:365–71.